

Carbon Monoxide Oxidation on Pt-Ru Electrocatalysts Supported on High Surface Area Carbon

Flavio Colmati Jr., William H. Lizcano-Valbuena, Giuseppe A. Camara, Edson A. Ticianelli and Ernesto R. Gonzalez*

Instituto de Química de São Carlos, Universidade de São Paulo, CP 780, 13560-970 São Carlos - SP, Brazil

Este trabalho descreve a preparação e caracterização de ligas dispersas de Pt-Ru sobre carbono de alta área superficial, as quais foram avaliadas para a oxidação de CO em eletrodos de disco rotatório/camada fina porosa e para a oxidação de hidrogênio em células a combustível de eletrólito polimérico alimentadas com hidrogênio contendo 100 ppm de CO. Tratamentos térmicos (H_2 , 300 °C) aplicados aos catalisadores melhoram a tolerância a pequenas quantidades de CO e, em alguns casos, reduzem o potencial necessário para promover a oxidação de CO durante a varredura do potencial. Sob condições operacionais em uma célula a combustível na presença de CO, foi observado que os melhores resultados foram obtidos quando a liga Pt-Ru/C foi preparada por redução simultânea dos íons Pt (IV) e Ru (III), diferentemente da redução sequencial.

This work describes the preparation and characterization of Pt-Ru alloys dispersed on high surface area carbon, which were evaluated for CO oxidation on thin porous coating rotating disk electrodes and for hydrogen oxidation on polymer electrolyte fuel cells fed with hydrogen containing 100 ppm CO. A thermal treatment (H_2 , 300 °C) applied to the catalysts improves the tolerance to small quantities of CO and, in some cases, reduces the potential necessary to promote the CO oxidation during a linear potential scan. Under operational conditions in a fuel cell in the presence of CO it was observed that the best results were obtained when the Pt-Ru/C alloy was prepared by simultaneous reduction of the ions Pt (IV) and Ru (III), as opposed to a sequential reduction.

Keywords: carbon monoxide, Pt-Ru alloys, supported catalysts, thermal treatment

Introduction

In recent years there has been a steadily growing concern with the degradation of the environment and the effect of pollutants on human health.¹ High levels of pollutants are produced by internal combustion engines, particularly those running on diesel, in large urban centers. Today, the use of clean energy sources is considered an urgent necessity and, among the alternatives, fuel cells are attracting much interest.² In particular, polymer electrolyte membrane fuel cells (PEMFC), are considered good candidates for transportation and portable applications because they are capable of delivering high power densities and can start operating at room temperature.

In spite of the efforts to develop the direct methanol fuel cell (DMFC), which has the advantage of using a liquid fuel, the most efficient low temperature fuel cells still use

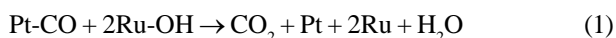
hydrogen as fuel. The cheapest way of producing hydrogen is by reforming fossil fuels or low molecular weight alcohols.³ This process produces 6-7% CO, which can be reduced to 1-2% by a shift reaction and to levels smaller than 100 ppm by partial oxidation.⁴ This CO adsorbs strongly on the Pt catalyst of the fuel cell electrode inhibiting the anodic reaction. The DMFC is not free of this problem, because the oxidation of methanol on Pt produces CO as an intermediate.⁵ The possibility of using PEMFC in transportation applications is a strong reason to search for solutions of the CO poisoning problem. For the DMFC a solution of this problem would allow to obtain power densities over 0.3 W cm⁻², necessary to make the fuel cell powered car competitive.

When impure hydrogen is used as a fuel, several approaches have been tested to make PEMFC's run with up to 100 ppm CO.⁶⁻¹⁹ These involve: i) adding small amounts of oxygen (up to 5%) to the hydrogen entering the anode,⁶⁻⁷ ii) performing a catalytic oxidation using Co

* e-mail: ernesto@iqsc.sc.usp.br

oxide,⁸ iii) using in the anode Pt alloys with other metals like Ru,⁹⁻¹³ Sn,¹⁴ Rh,¹⁵ Mo,¹⁶ Re,¹⁷ or some noble metals like Au¹⁸ and iv) using Pt-Ru alloys and adding small amounts of hydrogen peroxide, as an oxygen carrier, to the water hydrating the membrane.^{19,20}

Although some reports point to the Pt-Mo alloy as being the more effective,²¹ Pt-Ru alloys have been more extensively investigated. The use of Pt alloys is based on the fact that the less noble metal forms the hydrated oxides necessary to oxidize CO at lower potentials. Thus, the CO adsorbed on Pt is oxidized by the second metal through the so-called bifunctional mechanism:²²



In order to understand better the oxidation of CO to CO₂ several studies have been carried out on the adsorption of CO on Pt, using techniques as FTIR²³ and DEMS.²⁴ It is observed that CO adsorbs on Pt in two forms: bridge and linear bonding.^{25,26} Morimoto *et al.*²⁷ used *in situ* FTIR and cyclic voltammetry (CV) to study the characteristics of the adsorption of CO on surfaces with different morphologies. They found that on smooth surfaces the bridge form amounts to 12%, while for rough surfaces this figure increases to 29%.

Ianiello *et al.*²⁸ studied the oxidation of CO on smooth Pt and Pt-Ru alloys by *in situ* FTIR identifying the OH species that participate in the process. The lowest oxidation potential was found for the 50:50 Pt-Ru material. A similar result was presented by Arico *et al.*²⁹ for Pt-Ru alloys supported on carbon. On smooth rotating disk electrodes (RDE) Gasteiger *et al.*⁹ proposed that the oxidation of CO on Pt-Ru follows a Langmuir-Hinshelwood mechanism. Later, Schmidt *et al.*³⁰ proposed a method for the evaluation of catalysts for the oxidation of H₂ and CO by working with Pt and Pt-Ru particles supported on carbon and covered with a Nafion[®] film. A kinetic study of the oxidation of CO was presented later by the same authors.³¹ Recently, it was demonstrated in this laboratory that carbon supported Pt and Pt-Ru electrodes show a better performance for the oxidation of H₂ containing 100 ppm CO when submitted to a thermal treatment.³²

One of the electrochemical methods that has allowed a close study of certain electrode reactions on supported catalysts is the thin porous coating rotating disk electrode (TPC/RDE).³³ This technique was used for the study of oxygen reduction,³⁴⁻³⁶ and methanol oxidation³⁷ on carbon supported catalysts, allowing kinetic and mechanistic characterizations. In this work, the TPC/RDE technique was used to study the activity of several Pt-Ru/C electrocatalysts for the oxidation of CO prepared by

different methods which were eventually submitted to a thermal treatment in a hydrogen atmosphere. The catalysts that showed the better performances on the TPC/RDE system were also tested in single PEMFC operating with hydrogen containing 100 ppm CO.

Experimental

Carbon supported Pt-Ru catalysts were prepared by the following methods, using carbon powder (Vulcan XC-72) pre-treated as described elsewhere:³⁸

*Formic acid method (FAM)*³⁹

This method was developed in this laboratory and uses formic acid for the reduction of Pt and Ru. Developed initially as a simple method not requiring thermal treatments, it was found later that an adequate thermal treatment (here designed as T. T.) improves the performance of the catalyst for H₂/CO mixtures.³² For the preparation of Pt-Ru supported alloys freshly prepared aqueous solution of RuCl₃ as precursor were used, to avoid the formation of complexes RuO[(H₂O)₄]⁺² present in aged solutions of RuCl₃.

*Radmilovic et al. method (RM)*⁴⁰

It is similar to a method proposed earlier by Watanabe *et al.* (WM)⁴¹ but includes a thermal treatment in a hydrogen atmosphere at 300 °C for one hour.

In all cases the metal content with respect to carbon was 20% by weight. For the purpose of making comparisons, commercial carbon supported Pt and 50:50 Pt-Ru (E-TEK) catalysts were also used.

The composition of the prepared catalysts was examined by energy dispersive X-ray (EDX) analysis using a scanning electron microscope (DSM 960 Zeiss) with a 20 keV electron beam and provided with a microanalyser Link Analytical QX 2000 and a detector of SiLi.

The particle sizes of the catalysts were approximately evaluated by X-ray diffraction (XRD) using a URD-6 Carl Zeiss-Jena diffractometer. The X-ray diffractograms were obtained with a low scan rate of 0.05 degree s⁻¹ for 2θ values between 30 and 100°. The particle size determinations were made using the peak associated to the (220) face of the fcc platinum lattice at 2θ values between 60 and 80° with a scan rate of 0.02 degree s⁻¹. In all cases the incident wavelength (KαCu) was 1.5406 Å.

The electrochemical characterization of the catalyst materials was carried out using voltammetry and linear potential scans with the TPC/RDE, as described in previous

works.³⁴⁻³⁶ The TPC/RDE was constructed using a PTFE cylinder with a cavity 0.15 mm deep and 0.19 cm² area. The carbon supported catalyst was agglomerated with a 6% PTFE suspension (DuPont) and placed in the cavity. The cylinder was joined to a Pine Instrument AFMSRE rotating system with a control unit ASR2E. A reversible hydrogen electrode (RHE) was used as reference and a 2 cm² Pt foil as secondary electrode. The base electrolyte was 0.5 mol L⁻¹ H₂SO₄ (Mallinckrodt) prepared with purified water in a Milli-Q (Millipore) system. Electrochemical experiments were done with a EG&G PAR 273 potentiostat/galvanostat coupled to a personal computer, using the software M270 (EG&G).

Gas diffusion electrodes for single cells were prepared using a carbon cloth (Stackpole) purified by a thermal treatment at 450 °C followed by treatment with 0.5 mol L⁻¹ HNO₃ at 80 °C. On the carbon cloth, a diffusion layer consisting of carbon powder (Vulcan XC-72R, Cabot) and 15% PTFE was applied first. A catalytic layer containing Nafion[®] and Pt supported alloys for the anode and Pt/C for the cathode was brushed on the diffusion layer. In all cases the metal content was 0.4 mg cm⁻². The Nafion[®] content was 1.1 mg cm⁻². Membrane and electrode assemblies were prepared with a Nafion[®] 115 membrane (DuPont) by hot pressing the electrodes at 50 atm and 125 °C. Single PEMFC experiments were carried out galvanostatically at 85 °C with pure oxygen at 1.7 atm and humidified at 90 °C and with either pure hydrogen or hydrogen containing 100 ppm CO, at 2 atm and humidified at 100 °C.

Results and Discussion

EDX results

Table 1 shows the atomic composition of the different Pt-Ru/C catalysts employed in this work determined by EDX. The emitted radiation energies are $L\alpha = 9.441$ kV and $M = 2.048$ kV for Pt and $L\alpha = 2.558$ kV and $M = 0.461$ kV for Ru. Thus, the value of the L energy for Ru is near the value of the M radiation for Pt, and this may introduce errors. Table 1 shows the composition values determined. Some Pt-Ru/C catalysts, with an approximate composition 80:20 were prepared by either simultaneous or successive deposition of the metals on carbon. The amount of Ru was similar in both cases.

Previous results³² show that when the FAM method is used to prepare Pt-Ru/C catalysts it is very difficult to obtain alloy compositions with more than 30% Ru. On the other hand, catalysts prepared with the RM method allow the preparation of alloys with an atomic Ru content up to 50%.

Table 1. Composition (EDX), particle size (XRD) and cell parameter a (XRD) for the several Pt-Ru/C alloys

Pt-Ru atomic percentage	Particle size (nm)	Cell parameter a (nm)
100	2.9	0.39244
92:08 (s)	4.5	0.39103
92:08 (s) T. T.	7.8	0.39131
84:16 (s)	2.6	0.39121
84:16 (s)T. T.	2.9	0.39216
79:21 ^a	3.6	0.39188
79:21 T. T. ^a	4.7	0.39231
83:17 ^b	6.8	0.39058
83:17 T. T. ^b	9.3	0.39157
75:25 (s)	3.4	0.39107
75:25 (s) T. T.	4.5	0.39188
50:50 RM	5.0	0.38840 ^c
50:50 E-TEK	2.5 ^d	-

T. T. = material submitted to thermal treatment.

s = simultaneously anchoring of Pt and Ru; ^a Pt anchored first; ^b Ru anchored first; ^c From reference 40; ^d Unpublished TEM results.

XRD results

Figure 1 shows the diffractograms for the Pt-Ru/C catalysts prepared with the FAM. The peaks at $2\theta = 40, 47, 67$ and 82 are associated to the (111), (200), (220) and (311) planes, respectively, of the fcc structure of platinum,⁴² or a Pt-Ru phase rich in platinum that retains the fcc structure. It was not observed any peak due to metallic ruthenium or to materials rich in Ru with hexagonal structure. These structures would produce a peak at $2\theta = 44$, due to a reflection of the (101) plane, the most intense peak of hcp Ru, that could indicate their presence. However, it is known that for equal quantities of Pt and Ru the intensities of Ru peaks are lower than those of Pt peaks

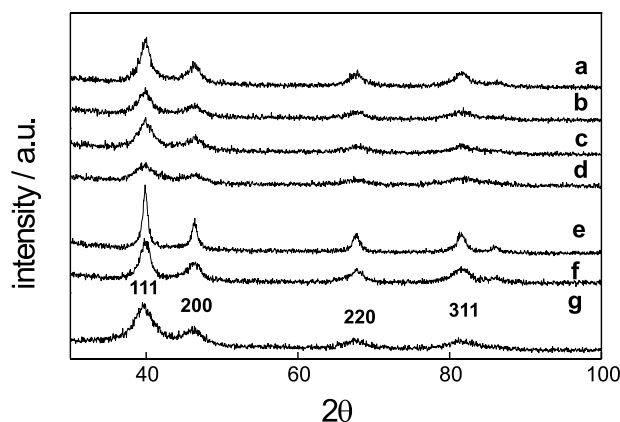


Figure 1. X-ray diffractograms for Pt-Ru/C FAM alloys with the metals anchored simultaneously. a) Pt-Ru/C 75:25 T. T.; b) Pt-Ru/C 75:25; c) Pt-Ru/C 84:16 T. T.; d) Pt-Ru/C 84:16; e) Pt-Ru/C 92:08 T. T.; f) Pt-Ru/C 92:08; g) (for comparison) Pt/C E-TEK. T.T.: thermal treatment.

and for this reason metallic Ru may not be detected in the carbon support. Also, it has to be taken into account that Ru is present in smaller amount than Pt and the peaks may be superimposed because of the broadening due to small particle sizes and the strain lattice effect.⁴³⁻⁴⁴

When the supported alloys were treated with H₂ for one hour at 300 °C it was observed that the peaks in the diffractograms become narrower, which could be due to: i) an increase in the crystallinity, ii) a lowering of the internal stress in the net of the alloy caused by a possible migration of Ru (as a substitution defect) or iii) an increase of the particle size. The same features are observed in the diffractograms of Figure 2, with the materials prepared by anchoring either Pt or Ru first. The profiles of the spectra were unchanged even when the catalyst powders were submitted to thermal treatment. In these cases it was expected to see the Ru peaks because the metals were anchored separately onto the carbon. However, no Ru peaks were observed probably due to the reasons discussed above. Figure 3 shows the diffractograms of the material prepared by the RM method and the commercial E-TEK electrocatalysts. For the RM material peaks associated to hexagonal Ru or species rich in Ru are not present, which suggests that in these materials the association between Pt and Ru is predominant. The diffractograms for the E-TEK alloys (Figure 3) are rather featureless, indicating either low crystallinity or very small particle sizes, preventing calculations of particle size or cell parameter.

Mean particle size

The mean particle size of the catalysts was determined from the X-ray diffractograms using Scherrer's equation⁴⁵ and assuming that the particles are spherical. In this case, the (220) peak of fcc platinum was chosen because it

appears in a region where the carbon substrate contributions can be removed, allowing a gaussian adjustment of the peaks to eliminate the background contributions. In order to obtain more precise measurements, the patterns for particle size determinations were obtained for 2θ between 60 and 80 ° with a scan rate of 0.02 degree s⁻¹. The mean particle sizes for all the materials used in this work are collected in Table 1. For the materials prepared with the FAM, particle sizes vary between 2.5 and 5 nm, being comparable to those resulting from other preparation methods. The particle sizes for catalysts prepared with the RM are close to those published by Watanabe *et al.* (3-4 nm)⁴¹ and Radmilovic *et al.* (1.9-2.3 nm).⁴⁰ Table 1 also shows that in all cases the particle size increases with the thermal treatment, probably due to sintering and agglomeration of the particles.

Cell parameter "a"

From the X-ray diffractograms, the cell parameter *a* was also determined for the catalysts used in this work, and the values are shown in Table 1. In all cases the values of *a* are smaller than those found for pure Pt (0.3923 nm), which indicates the presence of Ru substituting Pt in the lattice and leading to a smaller value of *a*. It must be noted that the value of *a* is slightly larger for the materials submitted to thermal treatment which may indicate some segregation in the alloy. Considering the Pt-Ru/C 80:20 alloy, the lattice parameter is smaller when both metals are anchored on the carbon particles simultaneously than when Pt is anchored first. This is a consequence of the presence of Ru in the fcc lattice of Pt, as further demonstrated by the still smaller value of *a* when Ru is anchored first. When the materials are thermally treated, the values of *a* for the catalysts obtained by simultaneous deposition and with

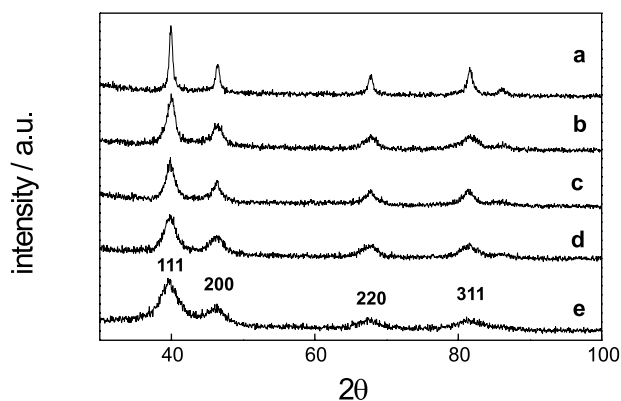


Figure 2. X-ray diffractograms for Pt-Ru/C 80:20 FAM with the metals anchored in succession. a) Ru-Pt/C T. T. b) Ru-Pt/C c) Pt-Ru/C T. T. d) Pt-Ru/C e) (for comparison) Pt/C E-TEK. T. T.: thermal treatment.

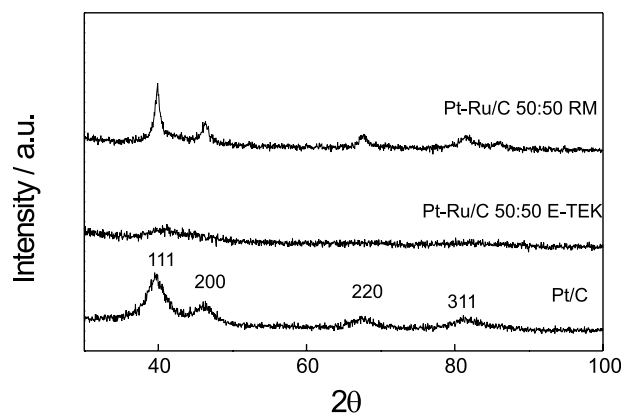


Figure 3. X-ray diffractograms for Pt-Ru/C alloys prepared by the Radmilovic method and commercial E-TEK electrocatalysts.

the previous deposition of Pt increase, approaching the value for pure Pt. On the other hand, the a parameter for the catalysts obtained with the initial deposition of Ru remains lower. In this case, a predominance of Ru in the lattice prevails, even after the thermal treatment.

The values of a for materials prepared with the FAM are larger when compared with those of the catalysts obtained by other methods.^{40,41,46-48} Arc melted Pt-Ru alloys show $a = 0.3904$ nm for Pt-Ru 80:20 and 0.3864 nm for Pt-Ru 50:50, while this last composition has a value of 0.38965 nm when prepared by chemical reduction with sodium borohydride on a carbon support.⁴⁷ Radmilovic *et al.*⁴⁰ found 0.3898 nm for the 75:25 and 0.3884 nm for the 50:50 Pt-Ru/C alloys. Thus, this method seems to favor the formation of solid solutions more than the FAM. Recently, it was reported by Takasu *et al.*⁴⁸ that the Ru precursor used to produce the catalysts has an effect on the structure of the material. Thus, by using RuCl_3 to produce a Pt-Ru/C 50:50 alloy the value of a was 0.391 nm, similar to that found in this work. With $\text{Ru}_3(\text{CO})_{12}$ the values of a were 0.3882 and 0.390 nm for Pt-Ru/C 75:25 and 50:50 respectively, and with $\text{RuNO}(\text{NO}_3)_x$ the values were even smaller: 0.3862 and 0.3865 nm, respectively. The possible explanation for the low incorporation of Ru when RuCl_3 is used, is the formation of $[\text{Ru}(\text{CO})(\text{H}_2\text{O})\text{Cl}_4]^{-2}$ ⁴⁹ from RuCl_3 and HCOOH in solution when the reaction time is increased.

Electrochemical characterization of the catalysts

Cyclic voltammetry. Figure 4 shows cyclic voltammograms (CV) obtained with the TPC/RDE electrode for Pt-Ru/C 50:50 RM and Pt-Ru/C 50:50 and Pt/C from E-TEK.

The materials containing Ru do not present the peaks in the hydrogen region observed for pure Pt, which is due to the formation of Ru oxides at those potentials.⁵⁰ Also,

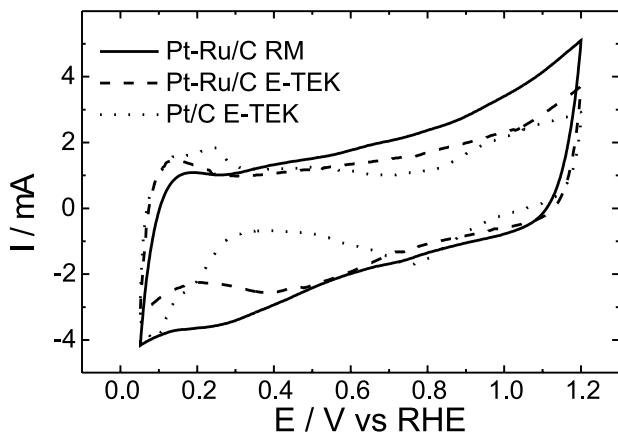


Figure 4. Cyclic voltammeteries for Pt-Ru/C 50:50 prepared by the RM and for Pt-Ru/C 50:50 and Pt/C E-TEK. $v = 10$ mV s⁻¹.

currents in the double layer are larger for these materials because of oxide formation. Some differences are apparent between the Pt-Ru/C E-TEK and the Pt-Ru/C RM. The former has a more characteristic hydrogen region and lower currents in the double layer region which is probably due to the different preparation methods. The Pt/C E-TEK material shows the typical behavior for this material in acid medium and it does not show the peak at 0.18 V due to the oxidation of hydrogen in the submonolayer.⁵¹

Figure 5 shows the CV's for the materials in which the metals were anchored simultaneously and separately by the FAM. Without any thermal treatment and when the metals are incorporated simultaneously (Figure 5A) the profile of the CV is that expected for an alloy in the sense that there is no definition of the hydrogen peaks. The profiles are slightly better defined when Ru was anchored first but the response is different from that of Pt/C E-TEK catalyst (Figure 5B). After the thermal treatment there are clear changes in the profiles that can be the result of: i) a reduced amount of Ru oxides, ii) segregation of Ru, iii) elimination of impurities, which may increase the area of the clean active surface and iv) an increase of particle size.

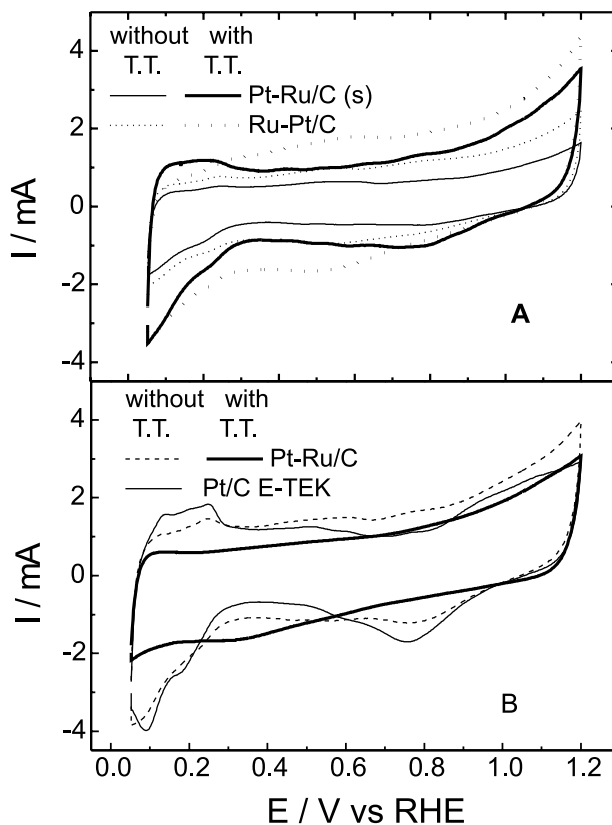


Figure 5. Cyclic voltammeteries of Pt-Ru/C 80:20 alloys prepared by the FAM, with and without thermal treatment (T.T.) (A) For the two metals anchored simultaneously (s) and Ru anchored first (Ru-Pt/C). (B) For the Pt anchored first (Pt-Ru/C) and, for comparison, for Pt/C E-TEK.

Effects (i-iii) are expected to increase the current, while effect (iv) should result in a decrease.

The thermal treatment results in a marked increase in the current levels for the material in which the metals were anchored simultaneously and for the material in which Ru was anchored first (Figure 5A). It is probable that, in spite of the increase in particle size, effects i-iii are predominant for these materials. The opposite must be the case for the material in which Pt was anchored first (Figure 5B) because a decrease of current levels is observed as a consequence of the thermal treatment.

Linear sweep voltammetry. The dependence of the amount of CO adsorbed with the electrode potential was studied by linear sweep voltammetry. In order to guarantee equilibrium conditions for the CO adsorption process with the TPC/RDE, the electrode was rotated at 1600 rpm for an adequate time. This was necessary because of the low solubility ($0.96 \times 10^{-3} \text{ mol L}^{-1}$) and diffusion coefficient ($1.8 \times 10^{-5} \text{ cm}^2 \text{ s}^{-1}$) of CO in $0.5 \text{ mol L}^{-1} \text{ H}_2\text{SO}_4$.⁹ Also, before applying the linear voltage scan it was necessary to eliminate the CO in the solution and in the pores of the TPC/RDE. This was done by bubbling N_2 with the electrode rotating at 1600 rpm until the response to the linear voltage scan was the same with and without rotation. Figure 6 shows a linear sweep voltammogram on Pt/C E-TEK for the oxidation of CO previously adsorbed at different potentials. Between 50 and 400 mV there is no dependence of the profiles on the potential at which CO was adsorbed. This is because at these potentials the CO is not oxidized on Pt, which needs the participation of adsorbed OH species formed at potentials above 0.7 V vs. RHE. Figure 7 shows the same experiment with Pt-Ru/C (50:50 E-TEK). In this case, the charge due to CO oxidation decreases slightly

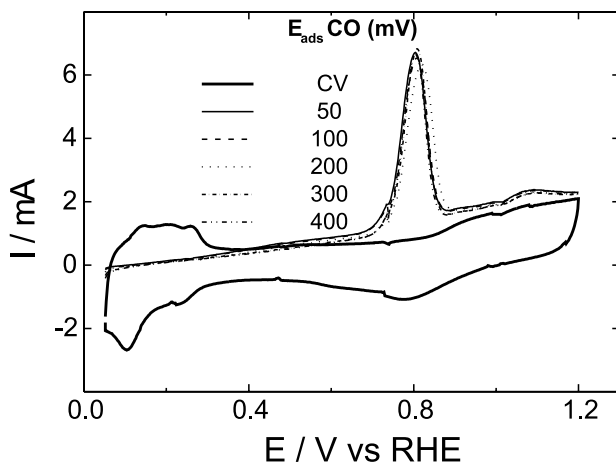


Figure 6. Stripping curves for CO oxidation on Pt/C E-TEK with adsorption of CO at several potential values indicated in the Figure in mV. $\nu = 10 \text{ mV s}^{-1}$. A cyclic voltammogram without CO is also included.

for increasing values of the CO adsorption potential. This is due to the oxidation of CO to CO_2 at potentials over 200 mV, induced by oxygenated species formed on Ru, and the extent of oxidation increases for increasing potentials. Because of this effect, all experiments were done adsorbing CO at 50 mV.

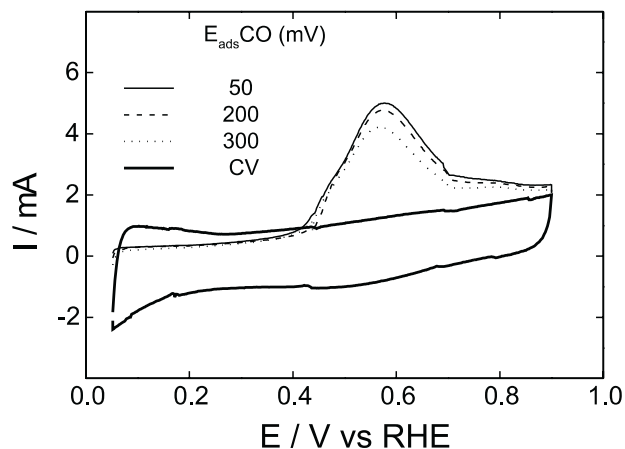


Figure 7. Stripping curves for CO oxidation on Pt-Ru/C 50:50 E-TEK with adsorption of CO at several potential values. $\nu = 10 \text{ mV s}^{-1}$. A cyclic voltammogram without CO is also included.

The stripping of CO on Pt presents an oxidation peak at a potential that depends on several factors. On the Pt/C electrodes used in this work, the peak potential is 0.815 V at 10 mV s^{-1} , which is much more positive than the value of 0.73 V observed on smooth Pt⁹ and platinumized Pt.⁵² Schmidt *et al.*³⁰ found a peak potential of 0.81 V at 20 mV s^{-1} on a thin supported catalyst electrode covered with Nafion[®], with no influence of diffusional effects, which agrees with the value of 0.80 V found on Pt (111) by the same authors. For scan rates of 50 mV s^{-1} other authors found a peak potential of 0.87 V.⁵³ As discussed by Schmidt *et al.*³⁰ the oxidation peak potential of CO on Pt nanoparticles appears around 0.81 V due to the fact that in small particles there is a predominance of (111) facets on the surface.^{40,54}

Figure 8A shows linear sweep voltammetry curves for the oxidation of CO on the Pt-Ru/C 80:20 catalysts prepared by the FAM and 50:50 prepared by the Radmilovic method. Also, the curves for the commercial catalysts Pt/C and Pt-Ru/C 50:50 E-TEK are shown. Neglecting double layer charging contributions, no currents are observed up to 0.2 V. On Pt/C a pre-wave can be observed between 0.20 and 0.75 V. This pre-wave was attributed to the oxidation of weakly adsorbed CO,⁵⁵ and it can also be seen up to 0.5 V on Pt-Ru/C materials (Figure 8A). Between 0.4 and 0.63 V the most active electrocatalyst is the commercial material Pt-Ru/C 50:50 E-TEK. Between 0.5 and 0.63 V the Pt-Ru/C 80:20 prepared by the FAM

and submitted to thermal treatment and the material prepared by the Radmilovic method present similar activity for the oxidation of CO. In spite of the improvement of the FAM material due to the thermal treatment the performance is not as good as that of the commercial E-TEK catalysts. Although a strict comparison cannot be made due to the differences in Ru content, it is probable that the better performance of the commercial material is due to a smaller particle size and a better Ru distribution on the surface of the electrocatalyst.

Figure 8B shows linear sweep voltammograms for the oxidation of CO on Pt-Ru/C 80:20 materials in which one of the metals was anchored first (Pt-Ru/C or Ru-Pt/C). It also shows the effect of the thermal treatment on these materials. The materials show some evidences of inhomogeneity. For example, in the material where Ru was anchored first, the peak at 0.5 V may be characteristic of CO oxidation on Ru particles.⁹ Without a thermal treatment, the alloy in which Pt was anchored first shows the best performance. That of the Ru-Pt/C material is poor, as is that of the material with simultaneous anchoring (Figure 8A). Evidently, the thermal treatment introduces qualitative changes in the performance

of the electrocatalysts for the oxidation of CO. The performance of the Ru-Pt/C material and that of the material with simultaneous anchoring show a marked improvement, while that of the Pt-Ru/C materials decreases somewhat. This is mainly the result of the combined effects of segregation of the materials and the increase in particle size due to sintering and agglomeration. The conclusion is that the Ru-Pt/C material with thermal treatment presents the lower potential for the oxidation of CO and currents comparable with those of the other materials.

The charge associated to the oxidation of CO, corrected for the double layer charging, was used to calculate the active areas of the catalysts and the values are presented in Table 2. The catalysts prepared by the FAM present an active area similar to that of Pt/C E-TEK, which is smaller than that of Pt-Ru/C E-TEK, probably due to the smaller particle size for this last material. For the catalysts prepared by the FAM, the thermal treatment promotes an increase in the active area, particularly for the material where the two metals were anchored simultaneously. This material without the thermal treatment presents active areas similar to those reported by Takasu *et al.*,⁴⁸ who found active areas of $34 \text{ m}^2 \text{ g}^{-1}$ for Pt-Ru/C materials prepared by impregnation using RuCl_3 as precursor.

Table 2. Electroactive areas of the different materials prepared by the FAM determined through the charge to oxidise a monolayer of CO. T.T.: thermally treated materials. The areas were normalized per g of Pt for all the catalysts

Catalysts	Electroactive area ($\text{m}^2 \text{ g}^{-1}_{(\text{Pt})}$)
Pt-Ru/C (s)	33.5
Pt-Ru/C (s) T.T.	58.0
Ru-Pt/C ^a	31.5
Ru-Pt/C T.T. ^a	44.6
Pt-Ru/C ^b	45.3
Pt-Ru/C T.T. ^b	48.4
Pt-Ru/C 50:50 E-TEK	66.5
Pt/C 100 E-TEK	56.0

(s): simultaneously anchoring of Pt and Ru; T. T.: Thermal treatment; ^a Ru anchored first; ^b Pt anchored first.

Experiments in single PEMFC

In order to extrapolate the results obtained with the TPC/RDE to practical systems, experiments were carried out in single PEMFC using Pt-Ru/C 80:20 catalysts prepared by the FAM. Figure 9 shows the performance of single cells operating with pure H_2 and with H_2 containing 100 ppm CO. The catalysts used in the gas diffusion electrodes were all thermally treated for 1 h in a H_2 atmosphere at 300°C . For comparison, Figure 9 incorporates results obtained with Pt/C and Pt-Ru/C E-TEK.

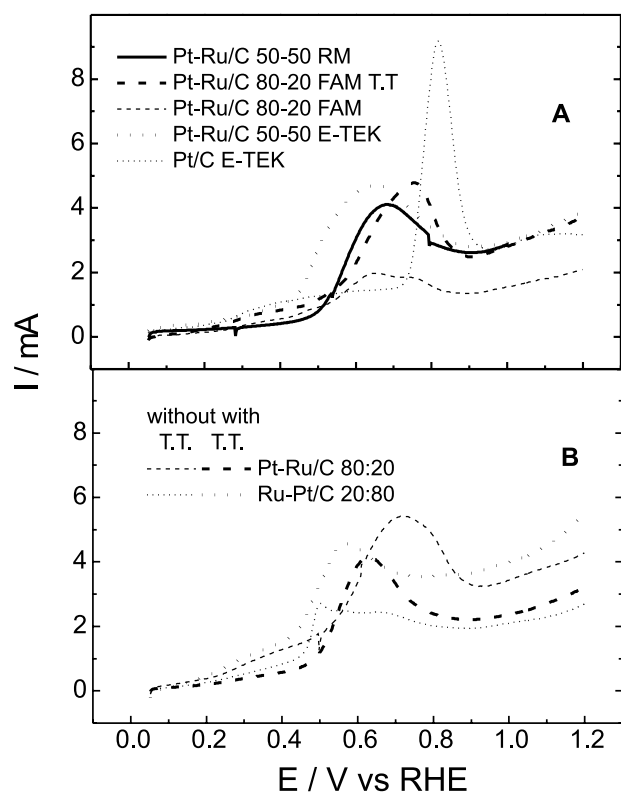


Figure 8. (A) Stripping curves of CO on Pt-Ru/C electrocatalysts, prepared by different methods, and E-TEK materials. Adsorption of CO at 50 mV vs RHE . $v = 10 \text{ mV s}^{-1}$. T. T.: thermal treatment. (B) Stripping curves of CO on Pt-Ru/C FAM electrocatalysts anchored in succession (with the order indicated in the material). Adsorption of CO at 50 mV vs RHE . $v = 10 \text{ mV s}^{-1}$. T.T.: thermal treatment.

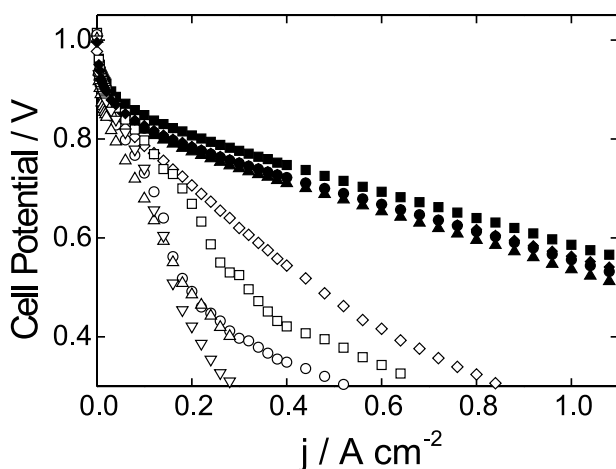


Figure 9. Curves E vs J in a single PEMFC operating with hydrogen (full symbols) or H₂/100 ppm CO (open symbols) using several electrocatalysts. (square) Pt-Ru (s) 80:20, (diamond) Pt-Ru/C 50:50 E-TEK, (circle) Pt-Ru/C 80:20, (up triangle) Ru-Pt/C 20:80 and (down triangle) Pt/C E-TEK.

When pure H₂ is used, the best results are obtained with catalysts in which Pt and Ru were incorporated simultaneously. The little differences in electrochemical performance for the different electrocatalysts can be associated to experimental errors because the oxidation of H₂ on Pt is very fast ($i_0 = 3.16 \text{ mA cm}^{-2}$ at pH=0).

When H₂ with 100 ppm CO is used in the anode there is, as expected, a large loss in performance for Pt/C. On the other hand, for Pt-Ru/C the loss is not so pronounced. In the region of low cd the losses are smaller probably due to the oxidation of weakly adsorbed CO. Again, the Pt-Ru/C material in which the metals were anchored simultaneously shows a better performance due to a smaller particle size and a larger active area as it was demonstrated by the calculation done from the charge necessary to oxidize a monolayer of CO. The thermal treatment affects the distribution of Ru and probably the material with simultaneous anchoring of Pt and Ru presents a better geometry at the molecular level for a bifunctional mechanism. When the two metals were incorporated separately, it makes no difference which metal is anchored first for the resulting active area (Table 2). For these materials, the increase in the active area with the thermal treatment is most probably due to a cleaning process of the catalysts as a consequence of the thermal treatment and possibly to a better distribution of Ru. The potential drop with current is lower for the 50:50 E-TEK Pt-Ru/C catalysts. A proper comparison with the FAM catalyst prepared here cannot be made because these present lower Ru contents and larger particle sizes. These results seem to confirm that for the oxidation of CO the best composition of the Pt-Ru alloy is 50:50.⁵⁶

Conclusions

The TPC/RDE showed to be suitable for the experimental evaluation of carbon supported catalysts and for studies of the mechanism of the reaction. With this technique it was possible to evaluate Pt-Ru/C catalysts prepared by different methods and submitted to different treatments for the oxidation of CO. Although the TPC/RDE technique showed differences in the results when one of the metals is anchored first, the results in single PEMFC were better for catalysts in which the two metals were incorporated simultaneously. A proper comparison of the materials prepared here with the commercial E-TEK catalysts could not be made because of the lower Ru content of the former.

Acknowledgements

Thanks are due to FAPESP, CNPq and FINEP (PRONEX), Brazil, for financial support. F.C.J. and W.H.L.V. thank FAPESP for research scholarships (98/10947-3 and 98/12922-8, respectively). The authors thank Vania Cardoso and Carlos Bento for the DRX and EDX experiments, respectively.

References

1. Du Melle, F. J.; *J. Power Sources* **1998**, *71*, 7.
2. Kordesch, K.; Simader, G.; *Fuel Cells and their Applications*, VCH: Weinheim, 1996.
3. Emonts, B.; Bogild Hansen, J.; Loegsgaard Jorgensen, S.; Hohlein, B.; Peters, R.; *J. Power Sources* **1998**, *71*, 288.
4. Twigg, M. V.; *Catalysts Handbook*, Frome: Manson, 1996.
5. Hamnett, A. In *Interfacial Electrochemistry. Theory, Experiment and Applications*; Wieckowski, A., ed.; Marcel Dekker, Inc.: New York, 1998.
6. Gottesfeld, S.; Pafford, J.; *J. Electrochem. Soc.* **1998**, *135*, 2651.
7. Gang, X.; Qinfeng, L.; Hjuler, H. A.; Bjerrum, N. J.; *J. Electrochem. Soc.* **1995**, *142*, 2890.
8. Teng, Y.; Sakurai, H.; Ueda, A.; Kobayashi, T.; *Int. J. Hydrogen Energy* **1999**, *24*, 355.
9. Gasteiger, H. A.; Markovic, N. M.; Ross, P. N.; *J. Phys. Chem.* **1995**, *99*, 8290.
10. Gasteiger, H. A.; Markovic, N. M.; Ross, P. N.; *J. Phys. Chem.* **1995**, *99*, 16757.
11. Gasteiger, H. A.; Markovic, N. M.; Ross, P. N.; Cairns, E. J.; *J. Phys. Chem.* **1994**, *98*, 617.
12. Morimoto, Y.; Yeager, E. B.; *J. Electroanal. Chem.*, **1998**, *441*, 77.
13. Oetjen, H. -F.; Schmidt, V. M.; Stimming, U.; Trila, F.; *J. Electrochem. Soc.* **1996**, *143*, 3838.

14. Shibata, M.; Furuya, N.; *J. Electroanal. Chem.* **1989**, *274*, 245.
15. Ross, P. N.; Kinoshita, K.; Scarpellino, A. J.; Stonehart, P.; *J. Electroanal. Chem.* **1975**, *59*, 177.
16. Grgur, B. N.; Zhuang, G.; Markovic, N. M.; Ross Jr, P. N.; *J. Phys. Chem. B.* **1997**, *101*, 3910.
17. Grgur, B. N.; Markovic, N. M.; Ross, P. N.; *Electrochim. Acta* **1998**, *43*, 3631.
18. Schmidt, T. J.; Gasteiger, H. A.; Behm, R. J.; *Abstract of the Workshop Electrocatalysis in Indirect and Direct Methanol PEM Fuel Cells. IIIrd International Symposium in Electrocatalysis*, Portoroz, Slovenia, 1999.
19. Schmidt, V. M.; Oetjen, H. F.; Divisek, J.; *J. Electrochem. Soc.* **1997**, *144*, L237.
20. Divisek, J.; Oetjen, H. -F.; Peinecke, V.; Schmidt, V. M.; Stimming, U.; *Electrochim. Acta* **1998**, *43*, 3811.
21. Mukerjee, S.; Lee, S. J.; Ticianelli, E. A.; McBreen, J.; Grgur, B. N.; Markovic, N. M.; Ross, P. N.; Giallombardo, J. R.; De Castro, E. S.; *Electrochem. Solid-State Lett.* **1999**, *2*, 12.
22. Watanabe, M.; Motoo, S.; *J. Electroanal. Chem.* **1975**, *60*, 275.
23. Iwasita, T.; Nart, F. C.; In *Advances in Electrochemical Science and Engineering*; Gerischer, H.; Tobias, C., eds.; VCH: Weinheim, 1995.
24. Wolter, O.; Heitbaum, J.; *Ber Bunsenges. Phys. Chem.* **1984**, *88*, 6.
25. Watanabe, M.; Motoo, S.; *J. Electroanal. Chem.* **1986**, *206*, 197.
26. Chang, S-C.; Weaver, M. J.; *J. Chem. Phys.* **1990**, *92*, 4582.
27. Morimoto, Y.; Yeager, E. B.; *J. Electroanal. Chem.* **1998**, *441*, 77.
28. Ianniello, R.; Schmidt, V. M.; Stimming, U.; Stumper, J.; Wallau, A.; *Electrochim. Acta* **1994**, *39*, 1863.
29. Arico, A. S.; Modica, E.; Passalacqua, E.; Antonucci, V.; Antonucci, P.L.; *J. Appl. Electrochem.* **1997**, *27*, 1275.
30. Schmidt, T. J.; Gasteiger, H. A.; Stab, G. D.; Urban, P. M.; Kolb, D. M.; Behm, R. J.; *J. Electrochem. Soc.* **1998**, *145*, 2354.
31. Schmidt, T. J.; Gasteiger, H. A.; Behm, R. J.; *J. Electrochem. Soc.* **1999**, *146*, 1296.
32. Castro Luna, A. M.; Camara, G. A.; Paganin, V. A.; Ticianelli, E. A.; Gonzalez, E. R.; *Electrochem. Commun.* **2000**, *2*, 222.
33. Tanaka, A. A.; Fierro, C.; Scherson, D.; Yeager, E. B.; *J. Phys. Chem.* **1987**, *91*, 3799.
34. Perez, J.; Tanaka, A. A.; Gonzalez, E. R.; Ticianelli, E.A.; *J. Electrochem. Soc.* **1994**, *141*, 431.
35. Calegario, M. L.; Perez, J.; Tanaka, A. A.; Ticianelli, E. A.; Gonzalez, E. R.; *Denki Kagaku* **1996**, *64*, 436.
36. Martins, S. A. M.; Perez, J.; Torresi, R. M.; Luengo, C. A.; Ticianelli, E. A.; *Electrochim. Acta.* **1999**, *44*, 3565.
37. Oliveira Neto, A.; Perez, J.; Napporn, W. T.; Ticianelli, E. A.; Gonzalez, E. R.; *Abstract of the Workshop Electrocatalysis in Indirect and Direct Methanol PEM Fuel Cells. IIIrd International Symposium in Electrocatalysis*, Portoroz, Slovenia, 1999.
38. Pinheiro, A L. N.; Oliveira Neto, A.; De Souza, E. C.; Perez, J.; Paganin, V. A.; Ticianelli, E. A.; Gonzalez, E. R.; *Abstract of the 2000 Fuel Cell Seminar*, Portland, USA, 2000.
39. Gonzalez, E. R.; Ticianelli, E. A.; Pinheiro A. L. N.; Perez, J., *Br INPI 00321*, **1997**.
40. Radmilovic, V.; Gasteiger, H. A.; Ross, P. N.; *J. Catal.* **1995**, *154*, 98.
41. Watanabe, M.; Uchida, M.; Motoo, S.; *J. Electroanal. Chem.* **1987**, *229*, 395.
42. Joint Committee on Powder Diffraction Standards, Powder Diffraction File, U. S. A., card 4-802.
43. Cullity, B. D.; *Elements of X-Rays Diffraction*, Addison-Wesley: Reading, 1978.
44. Hammond, C.; *Introduction to Crystallography*, Oxford University: Oxford, 1990.
45. West, A. R.; *Solid State Chemistry and its applications*, John Wiley & Sons: New York, 1984.
46. Arico, A. S.; Creti, P.; Kim, H.; Mantegna, R.; Giordano, N.; Antonucci, V. J.; *J. Electrochem. Soc.* **1996**, *143*, 3950.
47. Gurau, B.; Viswanathan, R.; Liu, R.; Lafrenz, T. J.; Ley, K. L.; Smotkin, E. S.; Reddington, E.; Sapienza, A.; Chan, B. C.; Mallouk, T. E.; Sarangapani, S.; *J. Phys. Chem. B.* **1998**, *102*, 9997.
48. Takasu, Y.; Fujiwara, T.; Murakami, Y.; Sasaki, K.; Oguri, M.; Asaki, T.; Sugimoto, W.; *J. Electrochem. Soc.* **2000**, *147*, 4421.
49. Seddon, E. A.; Seddon, K. R.; *The Chemistry of Ruthenium*, Elsevier: New York, 1984.
50. Ticianelli, E. A.; Beery, J. G.; Paffet, M. T.; Gottesfeld, S.; *J. Electroanal. Chem.* **1989**, *258*, 61.
51. Frelink, T.; Visscher W.; van Veen, J. A. R.; *J. Electroanal. Chem.* **1995**, *382*, 65.
52. Iúdice de Souza, J. P.; Iwasita, T.; Nart, F. C.; Vielstich, W.; *J. Appl. Electrochem.* **2000**, *30*, 43.
53. Feliu, J. M.; Orts, J. M.; Fernandez-Vega, A.; Aldaz, A.; *J. Electroanal. Chem.* **1990**, *296*, 191.
54. Stonehart, P.; *J. Appl. Electrochem.* **1992**, *22*, 995.
55. Herrero, E.; Feliu, J. M.; Aldaz, A.; *J. Electroanal. Chem.* **1996**, *368*, 101.
56. Gasteiger, H. A.; Markovic, N. M.; Ross, P. N.; Cairns, E. J.; *J. Phys. Chem.* **1993**, *97*, 12020.

Received: January 18, 2002

Published on the web: July 16, 2002

FAPESP helped in meeting the publication costs of this article.